Lithography-based ceramic manufacture (LCM) of auxetic structures: present capabilities and challenges

OPEN ACCESS
IOP Publishing
Smart Materials and Structures
Smart Mater. Struct. **25** (2016) 054015 (10pp)
doi:10.1088/0964-1726/25/5/054015

Lithography-based ceramic manufacture (LCM) of auxetic structures: present capabilities and challenges

Andrés Díaz Lantada[1], Adrián de Blas Romero[1], Martin Schwentenwein[2], Christopher Jellinek[2] and Johannes Homa[2]

[1] Product Development Lab, Mechanical Engineering & Manufacturing Department, Universidad Politécnica de Madrid (UPM), Spain
[2] Lithoz GmbH, Mollardgasse 85a/2/64-69, A-1060 Vienna, Austria

E-mail: adiaz@etsii.upm.es

Received 10 November 2015, revised 20 January 2016
Accepted for publication 25 January 2016
Published 8 April 2016

Abstract

Auxetic metamaterials are known for having a negative Poisson's ratio (NPR) and for displaying the unexpected properties of lateral expansion when stretched and densification when compressed. Even though a wide set of micro-manufacturing resources have been used for the development of auxetic metamaterials and related devices, additional precision and an extension to other families of materials is needed for their industrial expansion. In addition, their manufacture using ceramic materials is still challenging. In this study we present a very promising approach for the development of auxetic metamaterials and devices based on the use of lithography-based ceramic manufacturing. The process stands out for its precision and complex three-dimensional geometries attainable, without the need of supporting structures, and for enabling the manufacture of ceramic auxetics with their geometry controlled from the design stage with micrometric precision. To our knowledge it represents the first example of application of this technology to the manufacture of auxetic geometries using ceramic materials. We have used a special three-dimensional auxetic design whose remarkable NPR has been previously highlighted.

Keywords: auxetics, negative poisson ratio, metamaterials, additive manufacturing technologies, lithography-based ceramic manufacture

(Some figures may appear in colour only in the online journal)

1. Introduction

Conventional materials experiment a typical reduction in width when stretched. A quantitative measure of this dimensional change can be defined by a relevant property called 'Poisson's ratio' and defined as: $\nu = -d\varepsilon_{trans}/d\varepsilon_{axial}$, being ε_{trans} and ε_{axial} the transverse and axial strains when the material is stretched or compressed in the axial direction. In a more general case, ν_{ij} is the Poisson's ratio that corresponds to a contraction in direction '*j*' when an extension is applied in direction '*i*'. For most materials (and structures) the value of Poisson's ratio is positive and reflects a tendency to conserve volume. Auxetic materials (or metamaterials) are those with a negative Poisson's ratio (NPR), i.e. for displaying the unexpected property of lateral expansion when stretched, as well as a counterintuitive shrinking when compressed [1–6]. Natural auxetics (including some minerals, furs, skins…) and man-made ones (Gore-Tex®, polymeric foams) have been described and very special attention has been paid, since their discovery, to the search and development of auxetic structures designed and controlled even down to molecular scale levels [5–7].

It is important to highlight that auxetics, understood as materials and structures with a negative value of Poisson's ratio, are not only based on special geometries but also on special interactions with external and boundary conditions, including: negative pressure, proximity of certain phase transitions, specially inter-woven materials, living tissues and their extra-cellular environment, polydispersions, among other possibilities described in the seminal papers of this field [8–10, 11]. In any case, materials and structures leading to auxetic behavior are being progressively employed in the design of new products with interesting functionalities, especially in the area of shape morphing structures, expandable actuators and minimally invasive surgical tools and implantable devices. Regarding smart actuators based on an auxetic structure, it is important to cite some recent advances linked to auxetic shape-memory alloys for developing deployable satellite antennas [12] and some experiences linked to the characterization of polyurethane foams, with shape-memory behavior and auxetic properties, promoted thanks to several post-processing stages [13]. In the area of medical devices, recent studies have also assessed the behavior of a few auxetic structures for designing expandable stents [14–16] and their application to other surgical and implantable biodevices is clearly a matter of investigation. Several auxetic materials and potentially auxetic structures, normally grouped under the terms 're-entrant' (Almgren 1985), 'chiral' [17] and 'rotating' [18] in relation to the characteristics that promote the auxetic behavior, have been also summarized in previous comprehensive reviews.

In some studies just a scheme of their expected behavior and folding process, when submitted to uniaxial stresses, is drafted and provided, which proves to be limited for subsequent design activities. Recent comparative studies have tried to provide additional information of the more relevant properties of a wide set of auxetic structures, in order to assist with material/structure selection tasks for the development of novel auxetic-based smart structures and devices [19]. More recently, a comprehensive monograph, covering aspects linked to the micro-mechanical modeling of auxetics, to the elasticity of auxetic solids, to stress concentration, fracture and damage in auxetics, to contact and indentation mechanics of auxetic materials, and to overall mechanical, thermal and dynamic behavior of auxetics, has been published [23, 38].

Regarding the micro-manufacture of auxetic metamaterials, the first successful endeavor to obtain such geometries in the micro-scale, for achieving metamaterials with NPR, was performed using soft lithography, leading to details in the 100 μm range [24]. The lithographic process explained in such reference is interesting indeed and has helped to promote some appliances (i.e. micro-tubular structures as potential stents were analyzed).

However for adequately exploiting the potential of these auxetic metamaterials, an additional degree of precision is required. For instance, the manufacture of polymeric sheets with auxetic nano-structures can be useful indeed for the development of selective active membranes, whose pore sizes can be real-time controlled, just by applying uniaxial loads. Applications in areas including health (i.e. dialysis) and energy (i.e. membranes for catalytic reactors) are worth of investigation. By rolling such micro-/nano-auxetic sheets even easy-implantable devices (i.e. vascular stents) for minimally invasive surgery procedures can be obtained [24].

The fields of tissue engineering and biofabrication, with typical interactions at cellular and even molecular levels, can also clearly take advantage from auxetic metamaterials [25], especially if the preliminary experiences are further improved with the help of more micro- or nano-auxetics for obtaining even smaller clearances between the cells under culture. During cell culture, uniaxial excitations of an auxetic scaffold (or extra-cellular matrix) lead to biaxial expansions and compressions of the tissue being developed, which optimizes the control upon cell differentiation and promotes final tissue viability. Nevertheless, of the use of conventional micro-manufacturing resources for the development of quasi-2D auxetics and 3D auxetics, with typical distances between the lattices of the auxetic structure of more than 300 μm, leaves important clearances between cells and prevents interactions at cellular level.

Not just mechanical applications benefit from the special properties of auxetic metamaterials and take advantage from recently developed micro-manufacturing resources, but also auxetic-based systems for areas including optoelectronics and telecommunications require greater degrees of precision, than those achievable by traditional micro-machining facilities. Some additional remarkable procedures for developing real physical prototypes of mechanical metamaterials, with the finest details reaching hundreds of microns, include both subtractive approaches, i.e. laser ablation [26], and additive manufacturing (or 3D printing) procedures, such as laser stereolithography, digital light processing (DLP) or direct laser writing (DLW) [27, 28]. Usually, quasi-2D auxetic structures are manufactured resorting to surface micro-machining, laser ablation chemical etching, and other common mass-production processes imported from the electronic industry; while 3D auxetics, with more intricate geometries and inner details, can only be obtained by means of three-dimensional additive manufacturing or 'layer-by-layer' processes, including laser stereolithography, selective laser sintering or selective laser melting, among others. Promising approaches for the development of three-dimensional auxetic metamaterials and devices based on the use of DLW have been previously presented [29]. However, in spite of the attainable precision, the overall part size is still very limited for real-life and indsutrial applications and such process works more adequately just with polymers, which also limits the development of appliances for high-temperature environments.

Towards a more optimal compromise between part size, degree of precision and mechanical and thermal performance, shifting to high precision additive manufacturing technologies capable of working with ceramic materials seems to be an appropriate approach. In this study we present a very promising approach for the development of auxetic metamaterials and devices based on the use of lithography-based ceramic manufacturing (LCM). The process stands out for its precision and complex three-dimensional geometries

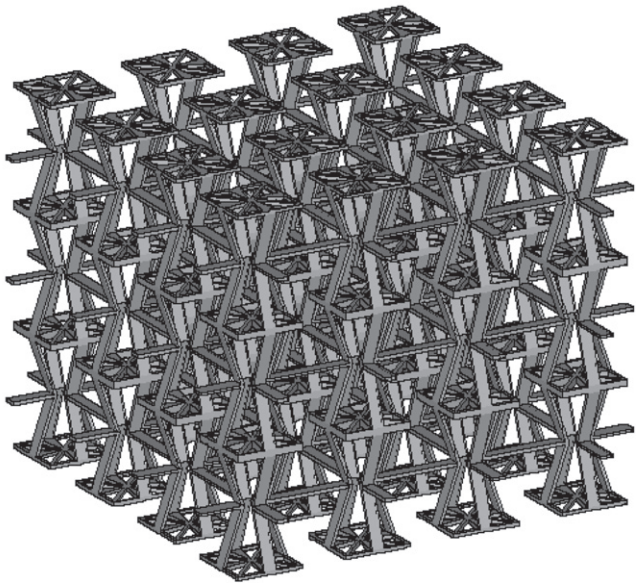

Figure 1. Three dimensional auxetic structure selected for present study.

attainable, without the need of supporting structures, and for enabling the manufacture of ceramic auxetics with their geometry controlled from the design stage with micrometric precision. To our knowledge it represents the first example of application of this technology to the manufacture of ceramic auxetics. We try to provide interesting details, in the following sections, regarding the design and manufacturing processes we have used, as well as some discussions about main results, present capabilities, difficulties and challenges towards nanoauxetics.

2. Materials and methods

2.1. Design and modeling process

The auxetic structure, used as case of study in this work, is designed using NX-8.5 (Siemens Product Life-cycle Management Solutions). First of all a unit cell is obtained and, subsequently, the use of Boolean operations and a three-dimensional matrix replication allow for the generation of a complete structure. In our case the cell unit is repeated four times in the x and y directions and three times in the z (vertical) direction, in order to obtain an almost cubic geometry. The repetitions are aimed at providing a clearer visual impression of the aspect of the auxetic structure or metamaterial, as sometimes, if using just one unit cell, it might be not so easy to visualize the global aspect. This three-dimensional auxetic is intended to experiment transversal contractions along x and y axes, when compressed along the z direction. In a similar way, tractions along the z direction may lead to transversal expansions.

Figure 1 shows the computer-aided design of the three-dimensional auxetic structure. The structure has been selected due its highly negative value of Poisson's ratio, which was previously reported [19]. In addition, due to having an intricate three-dimensional geometry, it can only be obtained using additive manufacturing technologies, which proves interesting for the technology being evaluated in this study. For this structure, the expected Poisson's ratio reaches a value of $\nu_{zx} \approx \nu_{zy} \approx -1.7$, when compressed along the z axis, which is perpendicular to the construction plane. The maximum geometrical volume reduction is around 17%, after application of the uniaxial loading levels that lead to the beginning of contacts between inner features, thus also promoting the beginning of buckling and structure collapse. The normalized Young's modulus (Young's modulus of the lattice structure/Young's modulus of the bulk material) reaches a value of 0.0002, according to previous results.

These results are again validated thanks to simulations carried using the finite element method, as described further on. They correspond also to values previously reported when testing upon macroscopic rapid prototypes obtained by laser stereolithography, although the ideal boundary conditions of the simulations are impossible to obtain in the real tests and the actual Poisson's ratios measured are typically around a 20%–25% lower than ideally expected [19]. Interestingly, there are some structures especially resistant to disorders and imperfections, which maintain their negative values of Poisson's ratio, even if the loads and boundary conditions are not ideal, such as happens with anti-chiral and chiral structures, as previously put forward [20–22], even though such structures are quasi-2D.

In any case, the validation of the actual properties when working with micro- and nano-auxetics is even more difficult, as the adhesion forces increase with part size reduction and the ideal boundary conditions, with free lateral displacements in the directions normal to the loading forces, are thus much more complicated to obtain. Uniaxial loading, using nanoindenters for example, prevents the ideally free lateral displacements because the whole upper and lower surfaces of the auxetics tend to adhere to the testing bench and the impact of such adhesion, being a surface force, increases with part size reduction. In addition, the microscopy facilities and procedures needed for adequately viewing the characterization process of a micro- or nano-auxetic, when using a nanoindenter, are beyond our reach. In consequence, in present study we just concentrate on design and manufacturing processes, while characterization of the actual behavior of such geometries remains a challenge for future research. As the mentioned properties (Poisson's ratio, maximum volume reduction and normalized Young modulus) are, in principle, scale-independent [1, 33], we hope that the provided simulated values may be useful for comparison purposes with future characterization results performed upon real prototypes, after solving the cited challenging characterization issues.

The mechanical performance of the structure is evaluated with the help of FEM-based simulations and using the advanced simulation module of NX-8.5. From the different possibilities of NX-8.5 for carrying out FEM simulations, NX-Nastran solver and structural static analysis type (SESTATIC101) are selected. We apply an alumina with a Young's modulus of 350 GPa, with a density of 3900 kg m^{-3},

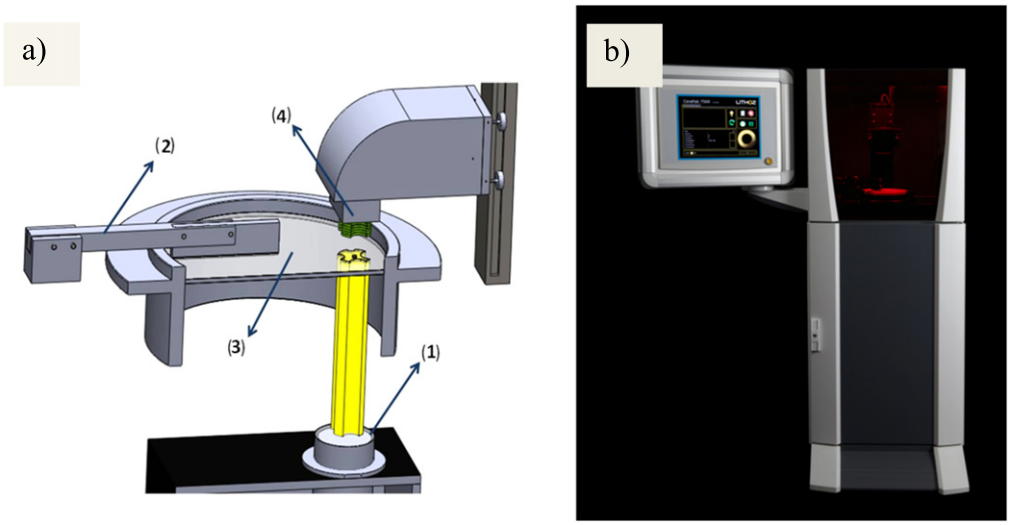

Figure 2. (a) Schematic image of the lithography-based ceramic manufacturing (LCM) process: (1) light source, (2) coating knife, (3) rotating vat filled with resin and (4) building platform. (b) Image of CeraFab 7500.

with a compressive strength of 2200 MPa and with a bulk Poisson ratio of 0.27. The structure is meshed using 4-node tetrahedral elements with at least two elements through thickness. The displacement along the vertical z-axis of the nodes at the base of the structure (corresponding to the XY construction plane) is fixed, leaving the lateral displacements free, so as to model an ideal auxetic performance. Increasing vertical displacements, along -z direction, are applied to the upper nodes of the structure. Four simulation cases are performed, with increasing values of applied deformation, including values of $\varepsilon_z = 0.325\%$; 0.65%; 0.975% and 1.3%, so as to evaluate the corresponding levels of stress and the attainable deformations and displacements. Convergence analyses are carried out using the h-method and the p-method. In the first case, the mesh is refined down to 0.5 μm size elements, thus adding more elements. In the second case, the complexity of the shape functions is increased by changing from 4-node tetrahedral elements to 10-node tetrahedral ones. Using both approaches the changes noticed, when comparing the stresses obtained for the different levels of deformation applied, are lower than 5%. Consequently, we consider the obtained results accurate enough for evaluation purposes.

2.2. Manufacturing process

Towards the desired degree of precision and performance, lithography-based additive manufacture of ceramics is probably the most suitable option. In short, lithograph-based additive manufacture of ceramics is based on the layer-by-layer selective curing of a photosensitive resin which contains homogeneously dispersed ceramic particles. The photopolymer acts as binder between the ceramic particles and makes the precise shaping of the part possible. The shaped form is produced as a green body that has to be further processed to obtain a part with higher relative density (99.85%–99.95%). These post-processing steps include the debinding, i.e. the thermal decomposition of the binder and the subsequent sintering into a compact ceramic part. This technology was developed at TU Wien [34, 35, 37] and is currently industrially developed by Lithoz GmbH.

2.2.1. Additive manufacture of master prototypes or green parts.

Once the design is prepared and optimized for 3D printing, manufacture is accomplished by means of LCM [36]. The master models or green parts are manufactured, with previously prepared alumina slurries, by DLP using the CeraFab 7500 machine, Lithoz GmbH (figure 2).

The slurries are prepared with commercial Al_2O_3 powders. These powders are homogeneously dispersed, with the help of a dispersing agent, in a formulation containing reactive monomers and a solvent. In addition, the formulation contains a photo-initiator (typically less than 1 wt%). The photoinitiator reacts under an external energy source, in this case a LED emitting at 460 nm, which excites the initiator, creating radicals that chemically react with the monomers included in the mixture. The chain reaction forms the desired matrix of (meth)acrylate monomers that bind together the ceramic particles in the shape of the original part. The reaction occurs in a brief lapse of time, while a determinate section of the part is being projected with specific intensity and exposure time parameters. DLP uses dynamic masks, which represent an individual cross section of the part being manufactured. The light engine uses high performance LEDs as light source and a DMD chip (digital mirror device) as dynamic mask with a resolution of 1920 $\times$ 1080 pixels and a pixel size of 40 $\times$ 40 μm.

The fabrication of the part is done in sequential layer-by-layer manner. For each individual layer fresh slurry is applied on the building envelope via a dosage system and subsequent rotation of the vat. Afterwards, the building platform is lowered into the dispersion to a distance of 25 μm to the bottom of the vat, which equals the thickness of an individual layer in the green body. Then the space-resolved exposure of the slurry is done by the projection of an image corresponding to the cross section of the current layer. Some images from

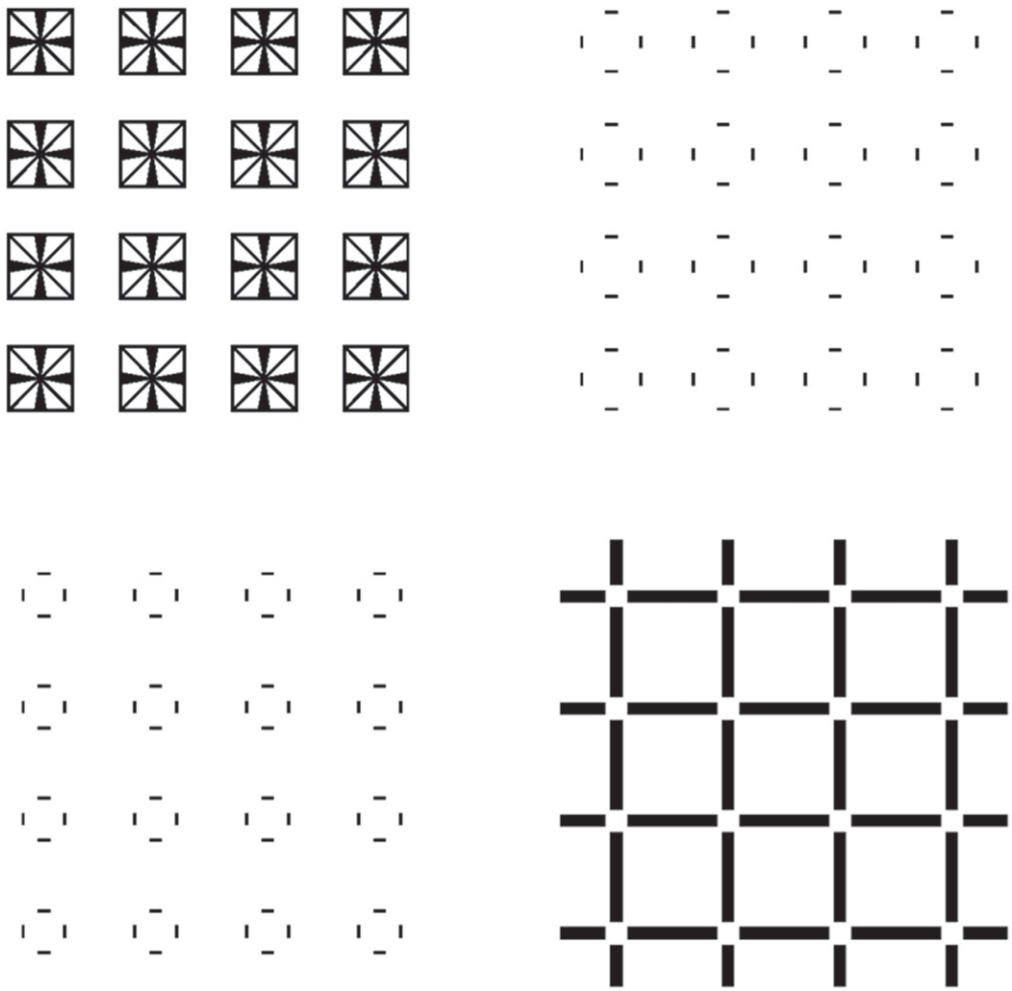

Figure 3. Some images from the mask-layers at various position during the printing.

the mask-layers are shown in figure 3 by means of example. After printing the parts, they are removed from the building platform. The green bodies are cleaned with solvent for several minutes until the non-polymerized slurry is removed from the cavities of the part.

2.2.2. Sintering towards final ceramic parts. The printed parts, once they are free of non-cured slurry, are subjected to a thermal treatment with the aim of obtaining a final ceramic solid part, free of any organic material. In addition, as the ceramic particles are separated, green parts have lower density and mechanical properties than compact alumina. The elimination of the organic components for achieving final composition and properties is carried out as described in previous research [37]. In short, the thermal variation is controlled inside a high-temperature chamber furnace from 30 °C up to 400 °C. Firstly, the solvent included in the slurry is evaporated.

Subsequently, a slow temperature variation is provided, so as to get an adequate decomposition of the binder, without causing internal stresses due to the formation of large amounts of gas at high temperature. In a second step, the

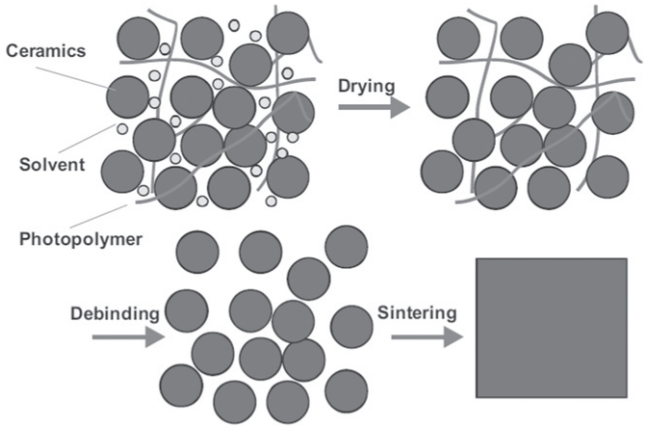

Figure 4. Steps of thermal treatment from the ceramic green body to the sintered dense ceramic.

Al_2O_3 particles are sintered. The part, already free of any organic component surrounding the ceramic particles, is raised up to 1600 °C, hence achieving sintering and resulting in a final compact part. The whole process is schematized in figure 4.

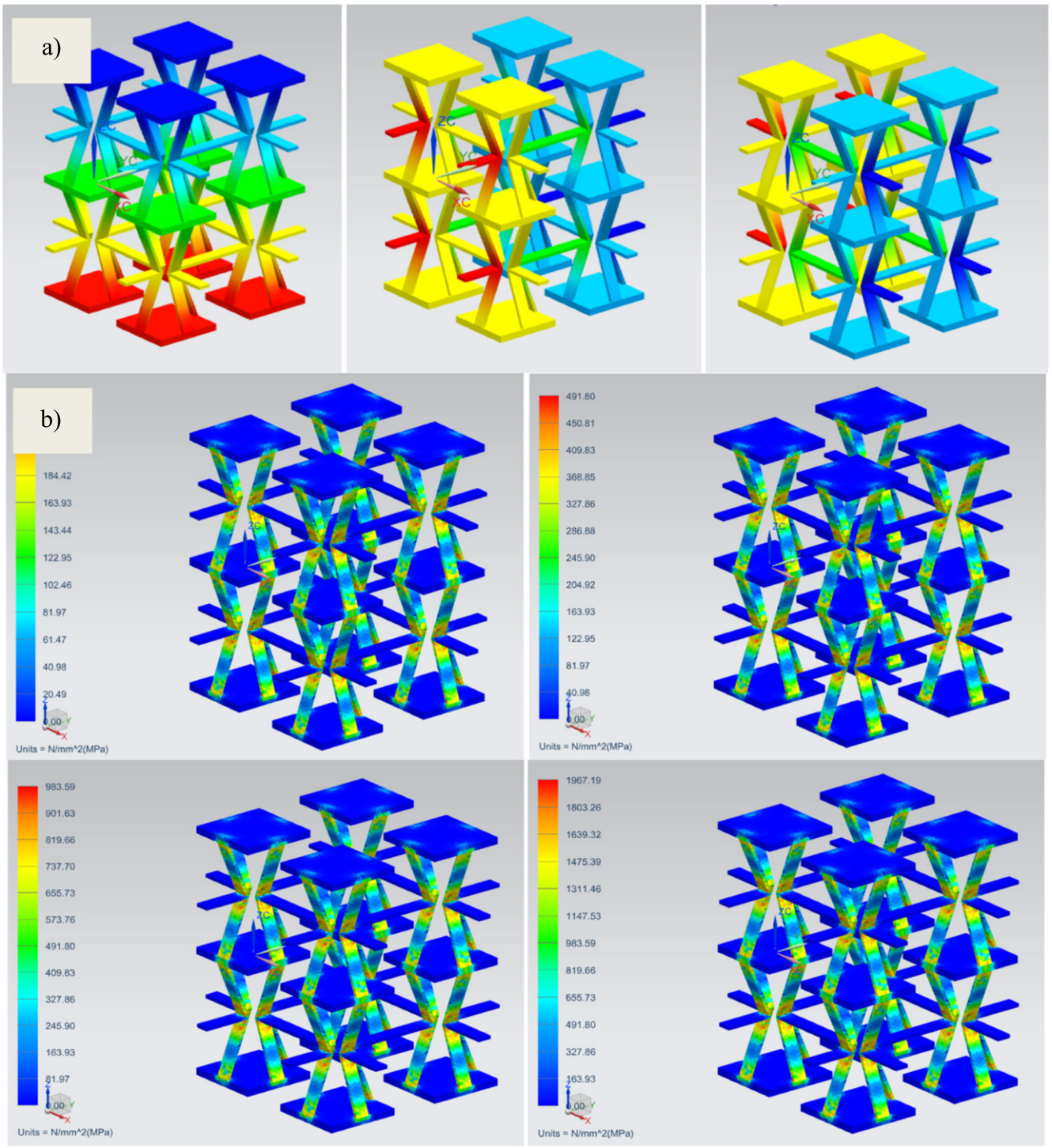

Figure 5. Finite-element method simulation results: (a) displacements results for verification of the Poisson's ratio. Represented in color-maps corresponding to displacements along *z*, *x* and *y* axes to highlight the symmetry present in the *XY* plane. (b) Stresses results corresponding to increasing levels of applied strain, so as to analyze the attainable degree of deformation before material's failure.

3. Results and discussion

Figure 5 shows the finite-element method simulation results, which help us to quantify the Poisson's ratio of the structure, which corresponds to previously studied values (Álvarez Elipe and Díaz Lantada, 2014), and to evaluate the attainable deformation levels, taking into account that the auxetic structure is obtained in a rigid ceramic. Figure 5(a) presents the displacements results for verification of a Poisson's ratio $\nu_{zx} = \nu_{zy} = -1.7$. They are represented in color-maps corresponding, respectively, to displacements along *z*, *x* and *y* axes to highlight the symmetry present in the *XY* plane. Figure 5(b) presents the stresses results corresponding to increasing levels of applied strain, so as to analyze the

attainable degree of deformation before material's failure. According to our results, the maximum level of deformation does not correspond to the geometrical limit, in which the trusses of the structure would start touching each other, but is limited to the stiffness and brittleness of the ceramic material. For deformation values of $\varepsilon_z = 1.3\%$, compressive stress values of 1900 MPa, just at the limit of the ceramic material, are obtained. The allowable deformations are clearly smaller than in auxetic foams manufactured using polymers, but still allow for displacements of 180 μm in our ceramic structures, which may be very appropriate for several application fields, as discussed towards the end of present section. Figure 6 shows the obtained auxetic model of 14 mm × 14 mm × 12 mm. Figure 6(a) shows the green parts or master models, just after the DLP photo-polymerization, while figure 6(b) shows the final sintered and compact ceramic structure. Details down to 20 μm and thicknesses lower than 200 μm can be appreciated in figure 5(c). Layers of 20 μm can be perceived. The models stand out for their symmetry and for the absence of inhomogeneous shrinking or structure collapse, which has been reported when using other high precision additive manufacturing procedures applied to auxetics [29]. To our knowledge, the manufactured example constitutes one of the more accurate ceramic lattices obtained following a predesigned geometry and, probably, the most complex and smallest auxetic geometry ever manufactured using a ceramic material.

Regarding the additive manufacture (3D printing) of auxetic materials previous pioneering studies have focused on the 3D printing, using fused-deposition modeling of thermoplastic polymers, of auxetic foams [30] and the use of additive manufacturing processes (laser stereolithography) for obtaining a mold for subsequent casting of silicone towards a final auxetic structure with very remarkable flexibility [31]. In terms of flexibility and attainable deformations of the auxetic structures, both approaches provide very interesting results and show potential for a wide set of applications. However, the use of conventional 3D printing, typically based on fused deposition modeling, or even the use of two-step processes combining a high precision technology and a subsequent casting procedure, are a bit more limited than our approach in terms of precision.

While previous 3D printed examples provide truss thicknesses down to 300–400 μm, the process used by our team leads to details smaller than 200 μm. In terms of the precision attainable, our previous experience with two-photon lithography [29] and that of colleagues with dip-in DLW [32] provide the highest level of detail attainable so far, although the overall size of the auxetic structure is compromised, which limits applicability. In fact, the structure by Bückmann and colleagues presents the important advantage of having the same Poisson's ratio along the three main directions, which converts it into a real three-dimensional dilational metamaterial [32], while the auxecticity of our structure is only remarkable when compressed or stretched along the direction perpendicular to the construction plane. However, to our knowledge, the presented auxetic structures, obtained by LCM, provide the best relationship between part size and degree of detail in the field of additive manufactured metamaterials.

In addition, although the deformations attainable with auxetic ceramics are much more limited, than using previously 3D printing approaches based on polymers, these ceramic metamaterials may be very interesting for a wide set of potential applications. First of all, many applications of auxetic materials may require only micrometric displacements and the additional stiffness of the base ceramic material used may be a positive property. For instance, for the development of high-frequency resonant structures (i.e. for antennae and telecommunication applications) or for interacting with micrometric precision (i.e. in cell culture processes and tissue engineering processes), the use of ceramic auxetics may be very appropriate, taking account of the fact that the material is osteoconductive and better in terms of biocompatibility, than most materials used for 3D printing. Furthermore, ceramics are much more resistant to higher temperatures, which may be of help for energy-related applications (i.e. in the development of active filters for turbomachinery). Their resistance to high temperatures, linked to their low thermal and electrical conductivities, may be useful for recently proposed applications of auxetics aimed at the control of deformations induced by gradients of temperature in shells, cylinders, spheres and plates (Lim, 2013). The control of stiffness, especially in sandwich structures [39], is also noteworthy. In fact, focusing on the control of thermal-induced deformations and of structure stiffness are some of the main keys for enabling additional specific applications of auxetics in several fields. Furthermore, three-dimensional auxetic structures have the potential to impact on a wide range of applications, from deployable and morphing structures to space-filling composites and medical treatments, and the properties of ceramics may benefit many of them.

Current challenges are linked to additionally improving the attainable degree of precision, while maintaining the capability of manufacturing large objects. The possibility of obtaining nanoauxteics can be useful for expanding the applications of these metamaterials. Nanometric details can even help to interact with micro-organisms, not just at a cellular, but also at a molecular level. Potential applications include the development of enhanced tissue engineering scaffolds, the manufacture of biological traps and the development of selective filters capable of capturing bacteria, viruses and pathogens for subsequent studies [25]. As the porosity of such structures can be changed by just applying uniaxial stresses, the related applications can be easily tuned and controlled in real-time, thus enabling novel methods for interacting with micro-organisms. The optimal biological properties of ceramic materials may result in improved performance.

Finally, it is also important to mention other remarkable, versatile, cheap and quite straight-forward manufacturing processes, capable of producing isotropic auxetic foams for a broad range of applications. The more relevant process is based on compression of a common foam structure, unstressing of the obtained structure without its modification and

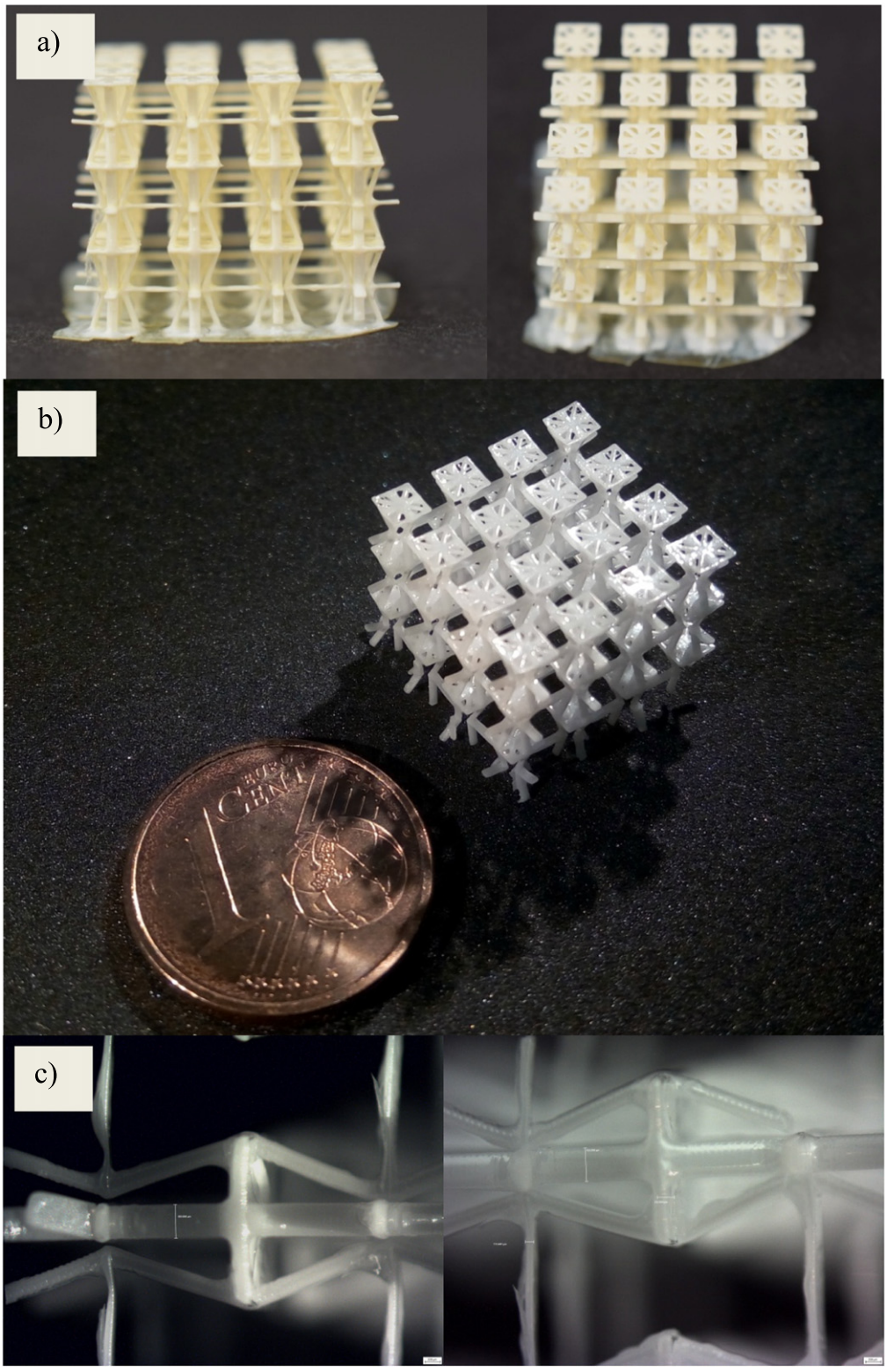

Figure 6. (a) Green part or master model just after digital light processing of the slurry. (b) Final result after sintering: auxetic ceramic structure with micrometric details obtained by means of lithography-based ceramic manufacture (LCM). (c) Detail of layers and unit cell.

'fixing' of the unstressed structure [40] and can be applied, not just to polymeric soft foams, but also to metallic materials [41], which helps to put forward its versatility. Additive manufacturing procedures, as the one LCM approach presented in this study, are clearly more expensive and may be time consuming, due to the need of an initial computer-aided design procedure.

However, in our opinion, the development of mechanical metamaterials, including auxetics, based on the combined use of computer-aided engineering resources and high-precision

additive manufacturing resources has important advantages, which can outperform other development processes, at least in some aspects. For instance, the possibility of defining concrete cell unit geometries and of replicating them to fill three-dimensional spaces is quite remarkable, especially taking into account that the finally manufactured prototypes exactly resemble the original design. Consequently, results can be controlled from the design stage. In addition, the use of Boolean operations for intersecting a designed metamaterial with an existing solid geometry, so as to manufacture a porous or lattice structure benefiting from the properties of the metamaterial, but with a pre-defined external geometry, constitutes a breakthrough with respect to mass produced foams. The use of computer-aided designs may even help to incorporate the metamaterial (or the auxetic) to a certain zone of a predesigned component, in order to incorporate some functionality to a concrete region of a device. Such knowledge-based designs, which may include gradients of mechanical, thermal, electrical and even optical properties, can be then obtained in a single step thanks to additive manufacturing resources.

4. Conclusions

In this study we have presented a very promising approach for the development of auxetic metamaterials and devices based on the use of LCM. The process stands out for its precision and complex three-dimensional geometries attainable, without the need of supporting structures, and for enabling the manufacture of ceramic auxetics with their geometry controlled from the design stage with micrometric precision. To our knowledge it represents the first example of application of this technology to the manufacture of ceramic auxetics. We have tried to provide interesting details, regarding the design and manufacturing processes we have used, as well as some discussions about main results, present capabilities, difficulties and challenges towards nanoauxetics.

Even though the progressive size reduction of artificially obtained auxetic geometries leads to real mechanical metamaterials and can promote novel applications, other difficulties linked to manipulation and integration into complex devices arise and further research is needed for taking advantage of these geometries. Future studies will be focused on the development of characterization procedures and support devices for addressing the actual auxetic behavior of the geometries obtained and for assessing the performance of ceramic auxetics.

We foresee relevant applications in several fields, such as biomedical and tissue engineering, i.e. for the development of active implantable medical devices, minimally invasive surgical actuators or active scaffolds for dynamic cell culture; aerospace and aeronautics, i.e. for the development of micro-actuators and highly accurate deployable structures; telecommunications and optoelectronics, i.e. for novel antennae designs, special photonic crystals and stress–strain electromechanical micro-sensors, among other interesting areas. Their use for controlling deformations induced by thermal gradients and for controlling stiffness of materials and structures is also noteworthy and may promote new applications in the already described fields of research.

We aim to continue our research searching for new appliances based on these interesting geometries and our geometries are at the disposal of colleagues who would like to further explore with us the potential of these geometries.

The described LCM process can be used for many other families of metamaterials and smart materials and structures, as a way of increasing the precision of available micro-actuators or micro-sensors based on the interesting properties of mechanical metamaterials.

Declaration of conflicting interests

Authors declare that no conflicting interests affected this research. Authors declare that no conflicting interests affected the objective presentation and description of results.

Acknowledgments

Present research was supported by the ‘Tomax: Tool-less manufacture of complex geometries’ project, funded by the EU Commission under grant agreement number 633192—H2020-FoF-2014-2015/H2020-FoF-2014 and led by Professor Dr Jürgen Stampfl from the Technical University of Vienna. We are indeed grateful for the detailed review and for reviewers’ comments and improvement proposals, which have helped us to incorporate interesting references, to take into account relevant issues and to enhance overall paper quality.

References

[1] Lakes R S 1987 Foam structures with a negative Poisson’s ratio *Science* **235** 1038–40
[2] Evans K E 2004 Auxetic polymers: a new range of materials *Endeavour* **15** 170–4
[3] He C, Liu P, McMullan P J and Griffin A C 2005 Toward molecular auxetics: main chain liquid crystalline polymers consisting of laterally attached para-quaterphenyls *Phys. Status Solidi* b **242** 576–84
[4] Liu Y and Hu H 2010 A review on auxetic structures and polymeric materials *Sci. Res. Essays* **5** 1052–63
[5] Wojciechowski K W 1987 Constant thermodynamic tension Monte Carlo studies of elastic properties of a two-dimensional system of hard cyclic hexamers *Mol. Phys.* **61** 1247–58
[6] Evans K E, Nkansah M A, Hutchinson I J and Rogers S C 1991 Molecular network design *Nature* **353** 124–124
[7] Griffin A C, Kumar S and Mc Mullan P J 2005 Textile fibers engineered from molecular auxetic polymers *NTC Project*: M04-GT21, 1-10, National Textile Center Report of 2004
[8] Wojciechowski K W 1989 Two-dimensional isotropic system with a negative Poisson’s ratio *Phys. Lett.* A **137** 60–4
[9] Hirotsu S 1991 Softening of bulk modulus and negative Poisson’s ratio near the volume phase transition of polymer gels *J. Chem. Phys.* **94** 3949–57

[10] Wojciechowski K W 2003 Non-chiral, molecular model of negative Poisson's ratio in two dimensions *J. Phys. A: Math. Gen.* **36** 11765
[11] Narojczyk J W and Wojciechowski K W 2010 Elastic properties of degenerate f.c.c. crystal of polydisperse soft dimers at zero temperature *J. Non-Cryst. Solids* **356** 2026–32
[12] Scarpa F, Jacobs S, Coconnier C, Toso M and Di Maio D 2010 Auxetic shape memory alloy cellular structures for deployable satellite antennas: design, manufacture and testing *EPJ Web of Conf.* **6** 27001
[13] Bianchi M, Scarpa F and Smith C W 2010 Shape memory behaviour in auxetic foams: mechanical properties *Acta Mater.* **58** 858–65
[14] Tan T W, Douglas G R, Bond T and Phani A S 2011 Compliance and longitudinal strain of cardiovascular stents: influence of cell geometry *J. Med. Devices* **5** 041002
[15] Gatt R, Caruana-Gauci R, Attard D, Casha A R, Wolak W, Dudek K, Mizzi L and Grima J N 2014 On the properties of real finite-sized planar and tubular stent-like auxetic structures *Phys. Status Solidi* b **251** 321–7
[16] Mizzi L, Attard D, Casha A R, Grima J N and Gatt R 2014 *Phys. Status Solidi* b **251** 328–37
[17] Prall D and Lakes R S 1997 Properties of a chiral honeycomb with a Poisson's ratio of −1 *Int. J. Mech. Sci.* **39** 305–14
[18] Grima J N and Evans K E 2000 Auxetic behaviour from rotating squares *J. Mater. Sci. Lett.* **19** 1563–5
[19] Álvarez Elipe J C and Díaz Lantada A 2012 Comparative study of auxetic geometries by means of computer-aided design and engineering *Smart Mater. Struct.* **21** 105004
[20] Pozniak A A and Wojciechowski K W 2014 Poisson's ratio of rectangular anti-chiral structures with size dispersion of circular nodes *Phys. Status Solidi* b **251** 367–74
[21] Gatt R, Brincat J P and Keith A 2015 On the effect of the mode of connection between the nodes and the ligaments in anti-tetra-chiral systems *Adv. Eng. Mater.* **17** 189–98
[22] Mizzi L, Attard D and Gatt R 2015 Influence of translational disorder on the mechanical properties of hexachiral honeycomb systems *Composites* B **80** 84–91
[23] Lim T-C 2015a *Auxetic Materials and Structures* (Berlin: Springer) (doi:10.1007/978-981-287-275-3)
[24] Xu B, Arias F, Brittain S T, Zhao X M, Grzybowski B, Torquato S and Whitesides G M 1999 Making negative Poisson's ratio microstructures by soft-lithography *Adv. Mater.* **11** 1186–9
[25] Soman P, Lee J W, Phadke A, Varghese S and Chen S 2012 Spatial tuning of negative and positive Poisson's ratio in a multilayer scaffold *Acta Biomater.* **8** 2587–94
[26] Alderson A, Rasburn J, Ameer-Beg S, Mullarkey P G, Perrie W and Evans K E 1999 An auxetic filter: a tuneable filter displaying enhanced size selectivity or defouling properties *Ind. Eng. Chem. Res.* **39** 654–65
[27] Kadic M, Bückmann T, Stenger N, Thiel M and Wegener M 2012 On the practicability of pentamode mechanical metamaterials *Appl. Phys. Lett.* **100** 191901
[28] Bückmann T, Stenger N, Kadic M, Kaschke J, Frölich A, Kennerknecht T, Eberl C, Thiel M and Wegener M 2012 Tailored 3D mechanical metamaterials made by dip-in direct-laser-writing optical lithography *Adv. Mater.* **24** 2710–4
[29] Hengsbach S and Díaz Lantada A 2014 Direct laser writing of auxetic structures: present capabilities and challenges *Smart Mater. Struct.* **23** 085033
[30] Critchley R, Corni I, Wharton J A, Walsh F C, Wood R J and Stokes K R 2013 The preparation of 3D auxetic foams by 3D printing and their characteristics *Adv. Eng. Mater.* **15** 980–5
[31] Babaee S, Shim J, Weaver J C, Chen E R, Patel N and Bertoldi K 2013 3D soft metamaterials with negative Poisson's ratio *Adv. Mater.* **25** 5044–9
[32] Bückmann T, Schittny R, Thiel M, Kadic M, Milton G M and Wegener M 2014 On three-dimensional dilational elastic metamaterials *New J. Phys.* **16** 033032
[33] Grima J N, Alderson A and Evans K E 2004 Negative Poisson's ratios from rotating rectangles *Comput. Methods Sci. Technol.* **10** 137–45
[34] Gruber H *et al* 2006 Rapid-prototyping method and radiation-hardenable composition of application thereto PCT/AT2006/000271, WO 2007002965 B1
[35] Patzer J F 2011 Generative Fertigung von keramischen Bauteilen für dentale Anwendungen *Dissertation* TU Wien
[36] Schwentenwein M and Homa J 2015 Additive manufacture of dense alumina ceramics *Appl. Ceram. Technol.* **12** 1–7
[37] Felzmann R, Gruber S, Mitteramskogler G, Tesavibul P, Boccaccini A R, Liska R and Stampfl J 2012 Lithography-based additive manufacturing of cellular ceramic structures *Adv. Eng. Mater.* **14** 1052–8
[38] Lim T C 2015b Thermal stresses in auxetic plates and shells *Mech. Adv. Mater. Struct.* **22** 205–12
[39] Grima J N, Oliveri L, Attard D, Ellul B, Gatt R, Cicala G and Recca G 2010 Hexagonal honeycombs with zero Poisson's ratio and enhanced stiffness *Adv. Eng. Mater.* **12** 855–62
[40] Pozniak A A, Smardzewski J and Wojciechowski K W 2013 Computer simulations of auxetic foams in two dimensions *Smart Mater. Struct.* **22** 084009
[41] Li D, Dong L and Lakes R S 2013 The properties of copper foams with negative Poisson's ratio via resonant ultrasound spectroscopy *Phys. Status Solidi* **250** 1983–7